Modeling of the Role of a Bax-Activation Switch in the Mitochondrial Apoptosis Decision

Chun Chen, Jun Cui, Haizhu Lu, Rui Wang, Shuai Zhang, and Pingping Shen
State Key Laboratory of Pharmaceutical Biotechnology, School of Life Sciences, Nanjing University, Nanjing, People's Republic of China

ABSTRACT We performed in silico modeling of the regulatory network of mitochondrial apoptosis through which we examined the role of a Bax-activation switch in governing the mitochondrial apoptosis decision. Two distinct modeling methods were used in this article. One is continuous and deterministic, comprised of a set of ordinary differential equations. The other, carried out in a discrete manner, is based on a cellular automaton, which takes stochastic fluctuations into consideration. We focused on dynamic properties of the mitochondrial apoptosis regulatory network. The roles of Bcl-2 family proteins in cellular responses to apoptotic stimuli were examined. In our simulations, a self-amplification process of Bax-activation is indicated. Further analysis suggests that the core module of Bax-activation is bistable in both deterministic and stochastic models, and this feature is robust to noise and wide ranges of parameter variation. When coupling with Bax-polymerization, it forms a one-way-switch, which governs irreversible behaviors of Bax-activation even with attenuation of apoptotic stimulus. Together with the growing biochemical evidence, we propose a novel molecular switch mechanism embedded in the mitochondrial apoptosis regulatory network and give a plausible explanation for the all-or-none, irreversible character of mitochondrial apoptosis.

INTRODUCTION

Systems biology is a hybrid experimental-computational approach. It takes a systemic view of cellular transactions caused by the interaction of the basic components of the cell. As an integral part of systems biology, mathematical modeling provides a unique opportunity for interweaving the individual molecules into an in silico fabric and dissecting complex networks into small elementary modules, thus helping to uncover the kinetic essences of different cellular transactions such as adaptations, oscillations, and switchlike phenomena (1–3). Various modeling methods have been implemented in recent years, including continuous ones employing numerical treatment of cellular information processing and discrete ones with excellent simplicity as well as scalability. Some of these methods are fully deterministic (4–6), while others have introduced noise (7–10).

Apoptosis is an all-or-none, irreversible physiological process through which the cell commits suicide when responding to various apoptotic stimuli (11,12). Once a cell has passed a certain checkpoint, it is fated to undergo apoptosis even after the stimulus has been withdrawn (13). These characteristics are believed to arise out of the apoptosis regulatory network.

Various models have focused on the mechanisms of apoptosis induction and have provided some elegant explanations. Bentele et al. (14) developed a model to explore the threshold mechanism for the regulation of CD95-induced apoptosis while Eissing et al. (15) modeled the process of receptor-induced apoptosis to show that interference of inhibitor of apoptosis (IAP and BAR) constitutes a bistable module. Another model raised by Bagci et al. (16) has demonstrated bistability caused by kinetic cooperativity in the formation of the apoptosome complex during mitochondria-dependent pathways. These models mainly focus on mitochondria-independent apoptosis, or concentrate on caspases which act downstream of mitochondria. However, little attention has been paid to mitochondrial regulatory events. It is widely recognized that mitochondrial regulatory events have priority in the cell fate decision. Mitochondrial outer membrane permeabilization (MOMP), which represents the ''point of no return'' of cell death, can commit a cell to die even when caspases are not activated (17). This raises the importance of uncovering the mechanism of mitochondrial regulatory events that play the crucial role in the apoptotic decision process. Another problem concerns the modeling methods. Models mentioned above are mostly based on ordinary differential equations (ODEs), which are deterministic descriptions in terms of concentrations and can only describe the average behavior of a system based on large populations. Also, the mass action law that underlies kinetic formulae is an approximation in which concentrations are assumed low enough to ignore the size of the molecules. It is now widely recognized that low copy numbers of molecules and macromolecular crowding effects in physiological conditions have to be taken into account in more realistic models (8,18). Recently, there has been an accelerating interest in the investigation of these effects in biological regulation through various kinds of stochastic modeling methods (10,19). Siehs et al. (20) did a pioneering job to simulate the apoptosis reaction network at mesoscale. They presented a cellular automaton (CA)-based simulation framework named Lattice Molecular Automaton (LMA), and successfully performed

Submitted October 17, 2006, and accepted for publication February 20, 2007.

C. Chen and J. Cui contributed equally to this work.

Address reprint requests to Pingping Shen, E-mail: ppshen@nju.edu.cn.

0006-3495/07/06/4304/12 $2.00

doi: 10.1529/biophysj.106.099606

discrete modeling of the role of interactions of Bcl-2 family proteins in governing the apoptosis decision. As they suggested, growing experimental knowledge about the apoptosis-relevant proteins would help to improve the model and further elucidate the regulatory mechanisms of apoptosis induction.

In this article, we translate acquired biological knowledge of the mitochondrial apoptosis regulatory network into mathematical models, in particular focusing on the regulatory events at the mitochondrial level. Two distinct modeling approaches were used for different purposes. Modeling by deterministic ODEs is convenient for bifurcation analysis and parameter discussion, while stochastic fluctuations and macromolecular crowding effects in cellular conditions are taken into account by stochastic CA modeling. Simulation results of these two methods support each other and reveal that a core module of Bax-activation is capable of displaying bistable behavior and forms a toggle-switch (bidirectional switch). With cooperation of Bax-polymerization, it changes to a one-way switch, strongly improving its robustness against stochastic fluctuations. Our simulation results, together with growing biochemical evidence, indicate that the bistable module of Bax-activation coupling with Bax-polymerization can form a bioswitch robust enough to govern the decision of mitochondrial apoptosis under noisy physiological conditions.

BIOLOGICAL BACKGROUND

Apoptosis is a well-regulated process, which is essential for tissue remodeling and homeostasis of multicellular organisms (21). Mitochondria play a crucial role in apoptosis by sensing incoming apoptotic signals and respond by mitochondrial outer membrane (MOM) permeabilization. Then, apoptogenic factors such as cytochrome *c*, Smac/DIABLO, and Omi/Htra 2 are released from the mitochondrial intermembrane space into the cytosol and nucleus, where they trigger caspase activation cascades and other cell-death events (22).

Although the exact molecular mechanism of MOMP is not elucidated, most experimental evidence indicates that MOMP is mainly governed by intricate interactions among Bcl-2 family proteins that possess either pro- or anti-apoptotic activities (23). The pro-apoptotic members are divided into two groups: the Bax group (Bax, Bak, and Bok) possesses BH1-3 domains, whereas the BH3-only proteins (Bid, Bad, Bim, Bik, Bmf, Puma, Noxa, and Hrk) share only the BH3 domain. The anti-apoptotic members as Bcl-2 and Bcl-xL contain all BH domains. In resting cells, some Bcl-2 family proteins (Bcl-2, Bcl-xL, and Bak) are targeted to MOM and other intracellular membranes, while others (BH3 only proteins, Bax) predominantly exist as soluble monomers or are sequestered by a number of non-Bcl-2 proteins in the cytosol (24).

Here we present a picture of the regulatory network of mitochondrial apoptosis (Fig. 1), which is mainly based on a switched rheostat model for the roles of Bcl-2 family proteins in regulating MOMP (25). Although it is reported that the occurrence of MOMP is sometimes independent of Bax, this is beyond the scope of our discussion in this article. Key events of our model were described as follows.

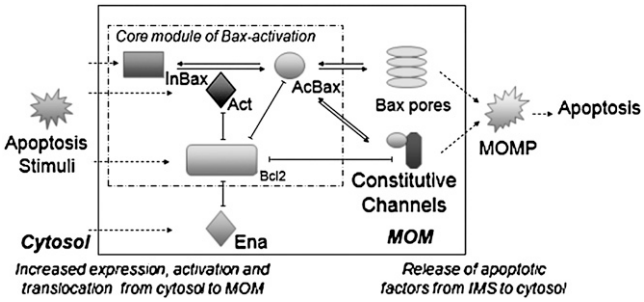

FIGURE 1 Outline of mitochondrial apoptosis regulatory network. We mainly focus on the roles of Bcl2 family proteins in regulating MOMP. Abbreviations of molecule names listed in Table 2 are used for clarity (e.g., Enabler (Ena), Activator (Act), inactive Bax (InBax), activated Bax (AcBax), etc.). Solid arrows denote reactions; dotted arrows describe subcellular translocation or upregulation; and those terminated by a bar denote interaction and inhibition. The dashed region indicates the core module of Bax activation.

Translocation of Bcl-2 family proteins from cytosol to MOM

In response to apoptotic stimuli, Bax monomers as well as BH3-only proteins translocate from the cytosol to MOM (24,26). Although the molecular mechanisms underlying these events remain incompletely understood, relocation of Bcl-2 family proteins from the cytosol to MOM can be regarded as the initial event of MOMP and apoptosis induction.

Activation of Bax and/or Bak

Recent evidence supports that select BH3-only proteins (Bid, Bim), which can be designated as ''Activator,'' are sufficient to enable a conformational change and pore formation of Bax/Bak (for general designation we use ''Bax'') through direct interaction with them (23,27,28). Anti-apoptotic family members (described as ''Bcl2'' for a general designation) can act as inhibitors by interacting with Activator and activated Bax (25,29–31). Other BH3-only proteins (Bad, Bik, Bmf, PUMA, Noxa, and Hrk) can act as ''Enabler'' by binding competitively to the anti-apoptotic family members, thus liberating the Activator and activated Bax (23,32). Activated Bax can spontaneously fall back to the inactive form, and perhaps relocate from MOM to the cytosol (13,33).

Pore formation and release of apoptogenic factors

The formation of mitochondrial apoptosis-induced channels (MAC) is thought to be the endpoint of the MOMP regulatory network (34). According to a report of Saito et al (35), activated Bax monomers can aggregate into tetramers to form

the protein-conducting channels. Furthermore, apoptosis-induced Bax/Bak clusters localized to MOM can be visualized by immunoelectron microscopy and they are tested to be responsible for MOMP (36). It is now widely accepted that Bax clusters consisting of four or more Bax monomers is responsible for conducting apoptotic factors such as cytochrome *c*. Moreover, the permeability of some constitutive channels (CC) on MOM, e.g., the voltage-dependent anion-selective channel (VDAC), can be regulated by Bcl-2 family members (37,38). Bax may trigger its conformational change resulting in VDAC opening for apoptogenic factors, while Bcl2 may have the opposite function.

MODEL AND METHODS

ODEs modeling

We developed a reduced model realizing mass action kinetics implemented as a set of ODEs, which is based on a simplified description of the mitochondrial apoptosis regulatory network. The ODE model can be dissected into three parts as follows:

1. Relocation of Bcl-2 family proteins from cytosol to MOM as initial signal. We suppose that the concentrations of Bax, Activator, and Bcl2 on the MOM increase linearly with the apoptotic stimulus, while details such as expression, degradation, and posttranslational regulation are not considered for reasons of simplicity (see Eqs. 1–4). F stands for the strength of the combined initial stimuli comprised of three parts, F_1, F_2, and F_3, which describe the effects of stimuli on the translocation of Bax, Activator, and Bcl2, respectively. The initial concentrations on MOM added to the translocated parts make up the mitochondrial concentrations of Bax, Activator, and Bcl2 (Bax_{mito}, Act_{mito}, and $Bcl2_{\mathrm{mito}}$ as indicated below), and the concentrations of translocated parts are in proportion to the stimuli F. Bax_{mito}, Act_{mito}, and $Bcl2_{\mathrm{mito}}$ are assumed to be constant during our simulations. Bax_{cytosol}, Act_{cytosol}, and $Bcl2_{\mathrm{cytosol}}$ represent the concentrations of Bax, Activator, and Bcl2 in the cytosol, respectively:

$$F = (F_1, F_2, F_3),\ F_1, F_2, F_3 \in [0, 1] \tag{1}$$

$$Bax_{\mathrm{mito}} = Bax_{\mathrm{initial}} + Bax_{\mathrm{cytosol}} \cdot F_1 \tag{2}$$

$$Act_{\mathrm{mito}} = Act_{\mathrm{initial}} + Act_{\mathrm{cytosol}} \cdot F_2 \tag{3}$$

$$Bcl2_{\mathrm{mito}} = Bcl2_{\mathrm{initial}} + Bcl2_{\mathrm{cytosol}} \cdot F_3. \tag{4}$$

2. Interaction network of Bcl-2 family proteins including: (*a*), activation of Bax by Activator in a kiss-and-run manner (23,27,28); (*b*), the inhibition of Activator and activated Bax by heterodimerization with Bcl2; and (*c*), a possible process in which activated Bax can replace Activator from Bcl2. The kinetics of these processes is described by the reactions and rate constants in Table 1. The rate equations of activated Bax monomer, free Activator, and free Bcl2 (the concentrations are indicated a [AcBax], [Act], and [Bcl2], respectively) are given in the following differential equations:

TABLE 1 Reactions and relative rate constants of ODEs modeling of the regulatory network of mitochondrial apoptosis

Description of reactions		
Act + InBax	$\rightarrow k_1$	Act + AcBax
AcBax	$\rightarrow k_2$	InBax
AcBax + Bcl2	$k_4 \rightleftharpoons k_3$	AcBaxBcl2
Act + Bcl2	$k_6 \rightleftharpoons k_5$	ActBcl2
AcBax + ActBcl2	$k_8 \rightleftharpoons k_7$	Act + AcBaxBcl2
4 AcBax	$k_{10} \rightleftharpoons k_9$	Bax_4

with

Rate constants	Initial conditions
$k_1 = 0.5\ \mu\mathrm{M}^{-1}\ \mathrm{s}^{-1}$	$Act_{\mathrm{mito}} = 0 \times 10^{-4}$ mM
$k_2 = 0.1\ \mathrm{s}^{-1}$	$Bax_{\mathrm{mito}} = 2 \times 10^{-4}$ mM
$k_3 = 2\ \mu\mathrm{M}^{-1}\ \mathrm{s}^{-1}$	$Bcl2_{\mathrm{mito}} = 1 \times 10^{-4}$ mM
$k_4 = 0.001\ \mathrm{s}^{-1}$	$Act_{\mathrm{cytosol}} = 1 \times 10^{-4}$ mM
$k_5 = 3\ \mu\mathrm{M}^{-1}\ \mathrm{s}^{-1}$	$Bax_{\mathrm{cytosol}} = 2 \times 10^{-4}$ mM
$k_6 = 0.04\ \mathrm{s}^{-1}$	$Bcl2_{\mathrm{cytosol}} = 0 \times 10^{-4}$ mM
$k_7 = 2\ \mu\mathrm{M}^{-1}\ \mathrm{s}^{-1}$	
$k_8 = 0\ \mu\mathrm{M}^{-1}\ \mathrm{s}^{-1}$	
$k_9 = 2\ \mu\mathrm{M}^{-1}\ \mathrm{s}^{-1}$	
$k_{10} = 0\ \mathrm{s}^{-1}$	

For clarity, abbreviations in Table 2 are used for description of reactions. We set k_{bcl2} (the rate of non-free Bcl2 shifting to free Bcl2; for details, see Model and Methods) equal to k_6 assuming that free Bcl2 originate from AcBaxBcl2 at the same rate with ActBcl2. The parameter k_1, k_3, k_4, k_5, k_6, k_8, and k_9 are set up to with one order-of-magnitude difference with respect to those used by Hua et al. (43) in their modeling of the effects of Bcl2-level on Fas signaling-induced caspase-3 activation. The ratio of k_3 to k_4 ensures an equilibrium constant of 1e-8M from (32), as well as those used for defining k_5 and k_6. The value of k_2, k_7, and k_8 are suitably chosen to reflect the experimentally known features (13,32,33). To reflect the irreversibility of the process of Bax-polymerization (35), k_{10} is step to 0 in our simulations. The concentrations of relative Bcl-2 family proteins in initial conditions are set up according to experimental data given by Kuwana et al. (42) and with one order-of-magnitude difference with respect to those used by Hua et al. (43).

$$\frac{d[\mathrm{Act}]}{dt} = -k_5 \cdot [\mathrm{Act}] \cdot [\mathrm{Bcl2}] + k_6 \cdot [\mathrm{ActBcl2}] + k_7 \cdot [\mathrm{AcBax}] \cdot [\mathrm{ActBcl2}] - k_8 \cdot [\mathrm{Act}] \cdot [\mathrm{AcBaxBcl2}], \tag{6}$$

$$\frac{d[\mathrm{Bcl2}]}{dt} = -k_3 \cdot [\mathrm{AcBax}] \cdot [\mathrm{Bcl2}] - k_5 \cdot [\mathrm{Act}] \cdot [\mathrm{Bcl2}] + k_{\mathrm{bcl2}} \cdot [\mathrm{Bcl2_{nonfree}}], \tag{7}$$

where $[\mathrm{Bcl2_{nonfree}}]$ indicates the total concentration of Bcl2 associated with both activated Bax and Activator ($[\mathrm{Bcl2_{nonfree}}] = [\mathrm{AcBaxBcl2}] + [\mathrm{ActBcl2}]$). We use k_{bcl2} to represent the rate of non-free Bcl2 shifting to free Bcl2, assuming that free Bcl2 originates from both Bcl2 non-free forms at the same rate. Also, the concentrations of proteins referred above should obey the following equations because of mass conservation:

$$\frac{d[\mathrm{AcBax}]}{dt} = k_1 \cdot [\mathrm{Act}] \cdot [\mathrm{InBax}] - k_2 \cdot [\mathrm{AcBax}] - k_3 \cdot [\mathrm{AcBax}] \cdot [\mathrm{Bcl2}] + k_4 \cdot [\mathrm{AcBaxBcl2}] - k_7 \cdot [\mathrm{AcBax}] \cdot [\mathrm{ActBcl2}] + k_8 \cdot [\mathrm{Act}] \cdot [\mathrm{AcBaxBcl2}], \tag{5}$$

$$[\mathrm{InBax}] + [\mathrm{AcBax}] + [\mathrm{AcBaxBcl2}] = Bax_{\mathrm{mito}}, \quad (8)$$

$$[\mathrm{Act}] + [\mathrm{ActBcl2}] = Act_{\mathrm{mito}}, \quad (9)$$

$$[\mathrm{Bcl2}] + [\mathrm{AcBaxBcl2}] + [\mathrm{ActBcl2}] = Bcl2_{\mathrm{mito}}. \quad (10)$$

According to Eqs. 8–10, substitutions and simplifications can be made for Eqs. 5–7, which ultimately employ [AcBax], [Act], and [Bcl2] as three variables of the differential equations. Equations 1–10 together give the mathematical representation of the core module of Bax-activation.

3. Bax-polymerization. Although the complete molecular identity of MAC is yet to be determined, activated Bax monomers are believed to aggregate into clusters that could represent protein-conducting pores (34,35). In our extended model considering Bax-polymerization, we suppose that tetramers are the sole form of Bax polymers equating to MAC. We use the following differential equation describing the kinetics of Bax tetramers (the concentration of Bax tetramers is indicated as $[\mathrm{Bax}_4]$, and the cooperative coefficient of Bax polymerization n is set to be 3):

$$\frac{d[\mathrm{Bax}_4]}{dt} = k_9 \cdot [\mathrm{AcBax}]^n - k_{10} \cdot [\mathrm{Bax}_4]. \quad (11)$$

Correspondingly, Eq. 5 describing the kinetics of activated Bax monomer and Eq. 7 describing the conservation of Bax are modified as follows:

$$\begin{aligned}\frac{d[\mathrm{AcBax}]}{dt} = {} & k_1 \cdot [\mathrm{Act}] \cdot [\mathrm{InBax}] - k_2 \cdot [\mathrm{AcBax}] - k_3 \cdot [\mathrm{AcBax}] \cdot [\mathrm{Bcl2}] \\ & + k_4 \cdot [\mathrm{AcBaxBcl2}] - k_7 \cdot [\mathrm{AcBax}] \cdot [\mathrm{ActBcl2}] + k_8 \cdot [\mathrm{Act}] \cdot [\mathrm{AcBaxBcl2}] \\ & - 4 \cdot k_9 \cdot [\mathrm{AcBax}]^n + 4 \cdot k_{10} \cdot [\mathrm{Bax}_4] \end{aligned} \quad (5')$$

$$[\mathrm{InBax}] + [\mathrm{AcBax}] + [\mathrm{AcBaxBcl2}] + 4 \cdot [\mathrm{Bax}_4] = Bax_{\mathrm{mito}}. \quad (8')$$

All the differential equations listed above were solved mathematically using the ODE23s routine of MatLab 6.5 (The MathWorks, Natick, MA). The simulation programs were written in M files, with commonly used MatLab subroutines. Bifurcation analysis was performed by using the subprogram AUTO contained in XPPAUT 5.91 (http://www.math.pitt.edu/~bard/xpp/xpp.html, Department of Mathematics, the University of Pittsburgh).

CELLULAR AUTOMATON

ODEs modeling usually has remarkable predictive power at macroscale levels, where molecules essentially lose their discreteness and become infinitely small and numerous. However, it always generates smooth curves that fail to capture the granularity or stochasticity of living systems. An alternative concept named the cellular automaton (CA) is presented here and specifically tailored to model mitochondrial apoptosis regulatory network. Its value for simulations of biological processes has been discussed previously (9,39). The crucial feature of the CA devised here is that it utilizes Brownian motion, which dominates over all other forces at mesoscale levels to mimic the movement of molecules on the MOM. A model considering all elements in Fig. 1 was carried out as a CA implementation, which is described as follows:

System representation

The MOM is realized on a two-dimensional, square lattice (four neighbors) with periodic boundaries. Each lattice site can contain a restricted number of molecules, according to the excluded volume effects in cellular conditions (40). Molecules are uniformly distributed on the lattice at the beginning of the simulation. They are supposed to be identical in size, but different weights that influence the abilities of molecules to move are taken into account. Characteristics of the various molecules are described in Table 2.

Brownian motion

In our implementation, the motions of all molecules are performed in a stepwise fashion. In each movement cycle, every molecule is first given a probability check, which determines whether it moves at this particular step due to its velocity (indicated by probability of movement in a step, given in the interval [0,100]; a velocity constant $V = 50$ means that the molecule has a probability $P = 50{:}100 = 0.5$ to move to a neighboring site per updated step). If a molecule is determined to be stationary in the probability check, an integer 0 is given to its movement direction. Otherwise, a random integer between 1 and 4, which indicates possible directions (up, down, left, and right, respectively) is designated. Next it passes a volume check to avoid violating the exclusion principle. A randomly chosen new direction is reassigned if its forth-going site has already been occupied completely. A movement step is finally performed and all molecules are moved according to their assigned velocities and directions.

Reaction rules

Reactions take place between two molecules occupying the same lattice site at a particular time step and follow simple pairwise interaction rules. If more than two molecules occupy a site, the reaction sequence is chosen in a random fashion. Reactions and rules are shown in Table 3, where the reaction rate constants are indicated by probabilities given in the interval [0,1000]. A reaction rate constant $K = 500$ means that probability of the reaction is $P = 500{:}1000 = 0.5$ per update step. Most reactions in our model are reversible. So, for molecules like dimers, a course of dissociation is included and a set of dissociation constants is embraced in the rules table. An exclusion check is employed to prevent extreme conditions when the designation of new molecules originated from old ones would violate the exclusion principle.

The CA modeling was implemented on a personal computer running Windows XP. Microsoft Visual Basic 6.0 was used as the programming language.

RESULTS AND DISCUSSION

Modeling of the mitochondrial apoptosis regulatory network

In our previous studies, we have constructed a simplified CA-based model of the mitochondrial apoptosis regulatory network, focusing particularly on two major mechanisms of how Bcl-2 family proteins regulate MOMP (41). Consistent with experimental results, our studies reveal that the

TABLE 2 Molecular table of CA modeling of mitochondrial apoptosis regulatory network

Abbreviations	Molecular descriptions	Weights	Velocities
Act	Activator	1	67
Bcl2	Bcl2	1	67
Ena	Enabler	1	67
ActBcl2	Heterodimer of Activator and Bcl2	2	50
EnaBcl2	Heterodimer of Enabler and Bcl2	2	50
InBax	Inactive Bax	1	67
$AcBax_m$	Activated Bax monomer/polymer (m represents the degree of polymerization of AcBax, e.g., $m = 2$ represent dimer of activated Bax, m can be omitted when $m = 1$)	m	0~67
AcBaxBcl2	Heterodimer of Activated Bax and Bcl2	2	67
CC	Constitutive channel	20	9
AcBaxCC	Activated Bax and Constitutive Channel Complex	21	9
Bcl2CC	Bcl2 and Constitutive Channel Complex	21	9
Other	Other molecules which have no reactions with Bcl-2 family proteins	1	67

Molecular weights of various kinds of proteins are assigned to discriminate the moving abilities of different molecules. The weights of Act, Bcl2, Ena, InBax, and Other are set up to 1, and the weights of CC is assigned a value bigger than Act, Bcl2, Ena, InBax, and Other according to experimental observations by Verrier et al. (37). Through calculating we can get the weights of other molecules like heterodimers and homopolymers. Molecular velocities (V) are assumed to be in inverse proportion to molecular weights (W) and they are calculated from $V = 100/(1 + W/A)$, where parameter A is used to regulate the inverse proportion relationship between W and V. We set $A = 2$ in our simulation and the values of relative molecules are listed in the velocities column of Table 2.

TABLE 3 Rules table of CA modeling of regulatory network of mitochondrial apoptosis

Descriptions of reactions		
Act + InBax	$\rightarrow K_1$	Act + AcBax
AcBax	$\rightarrow K_2$	InBax
AcBax + Bcl2	$K_4 \rightleftharpoons K_3$	AcBaxBcl2
Act + Bcl2	$K_6 \rightleftharpoons K_5$	ActBcl2
AcBax + ActBcl2	$K_8 \rightleftharpoons K_7$	Act + AcBaxBcl2
$AcBax_m$ + $AcBax_n$	$K_{10} \rightleftharpoons K_9$	$AcBax_{(m+n)}$*
Ena + Bcl2	$K_{12} \rightleftharpoons K_{11}$	EnaBcl2
AcBax + EnaBcl2	$K_{14} \rightleftharpoons K_{13}$	Ena + AcBaxBcl2
Ena + ActBcl2	$K_{16} \rightleftharpoons K_{15}$	Act + EnaBcl2
AcBax + CC	$K_{18} \rightleftharpoons K_{17}$	AcBaxCC
Bcl2 + CC	$K_{20} \rightleftharpoons K_{19}$	Bcl2CC
AcBax + Bcl2CC	$K_{22} \rightleftharpoons K_{21}$	AcBaxCC + Bcl2
With		
Rate constants		
$K_1 = 200$	$K_{10d} = 2$	$K_{17} = 350$
$K_2 = 6$	$K_{10t} = 1$	$K_{18} = 1$
$K_3 = 400$	$K_{11} = 500$	$K_{19} = 400$
$K_4 = 2$	$K_{12} = 1$	$K_{20} = 1$
$K_5 = 500$	$K_{13} = 150$	$K_{21} = 10$
$K_6 = 1$	$K_{14} = 150$	$K_{22} = 150$
$K_7 = 250$	$K_{15} = 250$	
$K_8 = 150$	$K_{16} = 15$	

An AcBax polymer can react with another to produce a lager AcBax polymer. In realistic reaction systems, the rate constants of Bax dimerization, trimerization, etc. must be different. We here make a simple assumption that larger polymers of AcBax are more likely to polymerize and the set of rate constants are defined by $K_9 = 1000 \times (m+n)/(B+(m+n))$. Here m, n, and $m+n$ are molecular weights of these polymers; B is a parameter to regulate the relationship between K_9 and $(m+n)$. We adopt $B = 10$ to make the value of K_9 comparable to other rate constants used in our CA simulation. Bax dimers and trimers are supposed to be able to dissociate and the dissociation constants are defined as K_{10d} and K_{10t}, respectively. The formation of larger Bax polymers is supposed to be irreversible. The parameters K_1 to K_9, K_{10d}, and K_{10t} are chosen to preserve the main ratio relationships among them in ODEs modeling. According to this set of parameters, K_{11} to K_{22} are chosen in such a way to realize stable dynamics on the simulation grid of our CA model as described by Siehs et al. (20).

concentration of Bax and the Bcl-2 to Bax ratio are key factors for controlling the MOMP and apoptosis. Here we extended this model by introducing more elements of the mitochondrial apoptosis regulatory network demonstrated in Fig. 1. The initial nonapoptotic condition of the mitochondrial system was simulated first and apoptotic stimuli were added to the system subsequently.

Initial nonapoptotic condition

We constructed the CA model at the single mitochondrion level. A grid of 100×100 squares is used to represent the outer membrane of the mitochondrion (~4 μm^2, calculated from the average size of a mitochondrion, so the size of each square is 20 nm × 20 nm). According to the excluded-volume effects, each square is restricted to containing five membrane proteins at most (as the diameter of membrane proteins is ~5–10 nm). Previous studies reveal that Bcl-2 family proteins have different concentrations in different cells as well as in different subcellular compartments (13,42). Kuwana et al. (42) calculated that tumor cells typically contain 200–600 nM Bax; other estimated concentrations are 25, 75, and 83 nM for Bid, Bcl2, and Bax, respectively (43). Some reports determined certain important ratios, such as Bcl-2 to Bax, which are critical for regulating the release of cytochrome c from the mitochondria (44,45). In particular, Childs et al. (46) quantified the amounts of mitochondrial Bcl-2 and Bax in rat cardiomyocytes using ELISAs and found that the ratio of Bcl-2/Bax is ~1.17, which is lifted to 1.41 upon administration of doxorubicin. Furthermore, estimating a cell volume of 1 picoliter shows that 1 nM = 600 molecules per cell, and according to Robin and Wong, a typical mammalian cell contains approximately several hundred mitochondria. Partly based on these data (the concentrations of relevant proteins, the average volume per cell, and the average number of mitochondria per cell), we made a rough estimate that there are 1600 Bcl2, 800 InBax, 200 Activator, 80 Enabler, 80 CC, and 3200 other proteins on the outer membrane of a mitochondrion in resting cells. These ''Other''

proteins help to simulate the crowded condition on MOM. Molecules are randomly scattered on the grid and after rapid diffusion and reactions, the system arrives at an equilibrium state that represents the initial condition of MOM in non-apoptotic cells.

Fig. 2 gives a snapshot showing the molecular information when the equilibrium state is achieved. Enabler and Activator are mostly sequestered by Bcl2 (Fig. 3 *a*, 0–1000 steps). The total number of Bax pores and active CCs are used to represent the occurrences of MOMP and apoptosis. Neither Bax pore (Bax tetramers and larger clusters) nor active CC (AcBaxCC) is found in this state (Fig. 3 *b*, the *dotted line* and *dashed line*, respectively, 0–1000 steps).

Simulating apoptosis induction

The amount of translocated Bcl-2 family proteins from the cytosol to MOM is used to represent the direct signal of apoptosis. Fig. 3, *a–c*, illustrates the effect of apoptotic signals on the homeostasis of the MOM system. At step 1000 the combined signal (including 2400 Bax, 250 Activator, and 120 Enabler) diffuses rapidly into the system. The number of Activator molecules decreases sharply after translocation because of Bcl2 sequestration (Fig. 3 *a*, *solid line*), but rises and maintains a high level in the next 3000 steps before falling down again, as does the Enabler (Fig. 3 *a*, *dotted line*). The number of AcBax monomers first rises sharply because of rapid activation (Fig. 3 *b*, *solid line*), but decreases because of Bcl2 sequestration later on. Then it rises again and maintains a relative high level. As AcBax aggregates into clusters at a later stage (Fig. 3 *b*, *dotted line*), the number of AcBax monomers finally drops. The amount

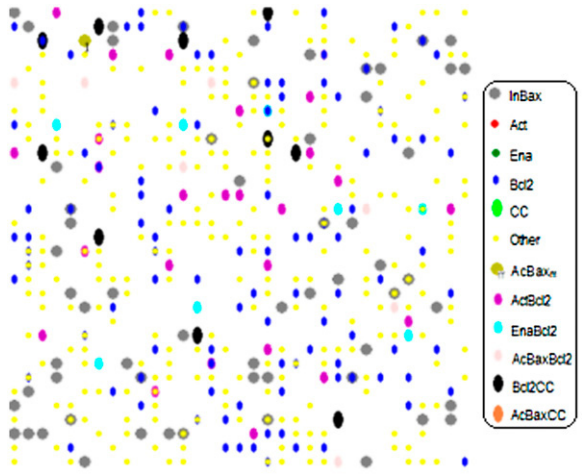

FIGURE 2 Snapshot of the CA simulation grid showing the coverage of different molecules when an equilibrium state of initial condition (non-apoptotic cells) is achieved. Given is only a section of the grid of 100×100 squares. Overlapping colors indicates that more than one molecule occupy a same lattice site at this particular time step. Molecules are indicated by distinct colors and shapes as described on the left. Abbreviations of molecule names listed in Table 2 are used for clarity.

of Bcl2 decreases at the early stage because of binding with both Activator/Enabler and AcBax monomers. However, after Bax-polymerization, Bcl2 is restored to a higher level (Fig. 3 *c*) and most Activator/Enabler molecules are sequestered again by Bcl2 (Fig. 3 *a*, *second decrease*). For comparison, similar kinetics of these molecules is plotted in Fig. 3, *c–e*, with a standard best-fit ODE modeling of these reactions. Notice that the CA kinetic curve displays stochasticity (or noise) compared to the one calculated by solving the ODEs. This stochasticity must be due to the randomness of molecule collisions when using a particle-based method, such as CA. Another reason for stochasticity is the reversibility of these reactions considered in our CA modeling. A slight difference between the curves of Bax pore exists in Fig. 3, *b* and *e*, because the processes of Bax polymerization are modeled using different expressions in CA and ODE model, respectively.

As shown in Fig. 3 *b*, after apoptosis induction, the number of Bax pores increases remarkably in contrast to active CCs. In this simulation, Bax pores constitute the major parts of the MACs, while active CCs play a negligible role. This is consistent with most experimental reports (34). However, in some reports active CCs such as VDAC and/or permeability transition pore complex have a dominant role in controlling MOMP (26,47,48). For example, in ethanol-induced apoptosis of rat hepatocytes, Bax was not found oligomerized but interacted with the mitochondrial channel protein VDAC, which is responsible for cytochrome *c* release and apoptosis (49). We do not yet know much about the molecular basis of the origin of these different behaviors. A natural explanation could be that the concentrations of relevant proteins are different in various cell and stimulus conditions. Our model provides opportunities to examine and test whether this assumption can work in theory. We changed the initial ratio of Bax to CC and relevant parameters in our simulation and consequently reversed the ratio of Bax pores to active CCs (Fig. 4). Here changing the reaction rate is equivalent to changing the concentrations of relative proteins. These results indicate that certain contradictory experimental results about the mechanism of MOMP may be due to different ratios of relevant proteins and parameters in various cell conditions. Nevertheless, we should admit that what we have proposed here is just a possible explanation and to further validate it, special examination of the concentrations of molecules and related wet-lab experiments under different conditions are needed.

We can also change the concentrations of molecules to study the roles of different Bcl-2 family proteins in the cell response to apoptotic stimuli. For instance, a twofold increase in the concentration of Bcl2 on MOM is used as initial condition in contrast to those in Fig. 3, *a–c*. Neither Bax pore nor active CC is observed during the whole simulation timescale (data not shown). So, we can conclude that in our model, a twofold increase in the concentration of Bcl2 on MOM can result in resistance to MOMP. This is consistent

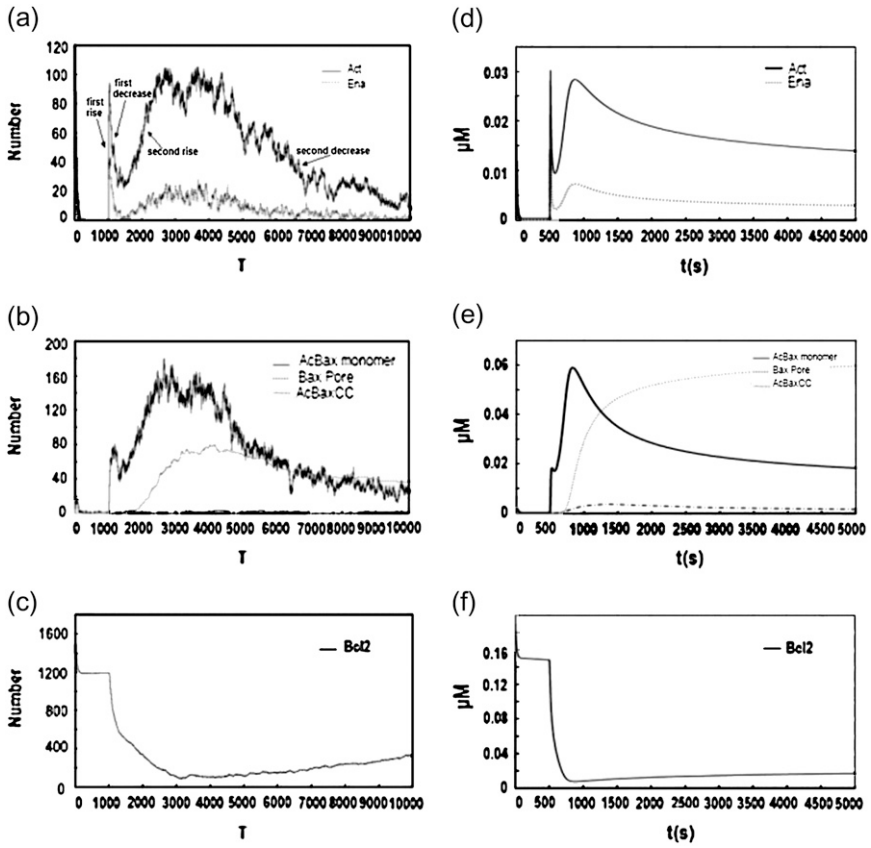

FIGURE 3 CA and ODEs modeling of the mitochondrial apoptosis regulatory network. The combined signal of apoptosis rapidly diffuses into the equilibrium system of initial condition. The concentration profiles of (*a*) Act, Ena, (*b*) AcBax monomer, Bax pore, and AcBaxCC, and (*c*) Bcl2 are plotted versus the CA time steps. For comparison reasons, similar kinetics of these molecules is plotted as panels *c–e* separately with a standard best-fit ODE modeling of these reactions.

with experimental reports in which Bcl-2 overexpressing cells are usually apoptosis-resistant (31,50). In our previous simplified model, by varying the concentrations of Bax and the Bcl-2-to-Bax ratio, these two factors were suggested to be key factors in regulating MOMP (41). Furthermore, the interaction rules of our CA model can be modified to perform experiments easily in silico. One consideration in the current study is that the process of Bax-activation is examined with the polymerization of activated Bax abolished.

Bax-activation: a core module of bistability

An important means to study a complex network is to dissect it into small elementary modules (1). The core module of Bax-activation was the initial focus. Experimental evidence suggests a self-amplification process of Bax/Bak-activation produced by BH3-only proteins (30,51). Cells can generate more activated Bax after initial activation of a few Bax molecules and there is always a lag between the initial Bax-activation and the first detectable MOMP. Bax/Bak auto-activation was proposed to be one possible explanation, although in vivo evidence is still lacking (51). An alternative explanation is based on the interaction network of Bcl-2 family proteins. Bax, Activator, and Bcl2 constitute a positive-feedback loop as shown in Fig. 1. Once Bax is activated, it can bind Bcl2 competitively to free Activator, which will in turn activate more Bax and amplify this process. In Fig. 3, *a* and *b*, the second increase of Activator and AcBax monomers indicates this self-amplification process. It is well known that nonlinear positive feedback can lead to bistability, a typical kind of bioswitch (52). This raises the question of whether the positive feedback here would be strong enough to make the core module of Bax-activation bistable.

ODE model

The core module of Bax-activation is first constructed using ODEs in a deterministic way (see Model and Methods). For simplicity, translocation of Activator is taken as the stimuli F ($F_1 = F_3 = 0, F_2$ varies from 0 to 1). We first performed bifurcation analysis with F as the bifurcation parameter (Fig. 5).

This module shows the desired bistability: two stable steady states coexist in a certain range of bifurcation parameter F, whereas outside this interval only a single steady state exists. As indicated in Fig. 5, there is an off-state in which the amount of total AcBax (monomer forms added to AcBax in polymer forms) is very low (near zero), and an on-state with a high level of Bax-activation. Another steady state exists between them but it is unstable and any perturbation will send this system either up to the on-state or down to the off-state. The arrows indicate the direction of evolution of the level of Bax-activation, starting from any region of the diagram.

To test whether bistability is an inherent character of the core module of Bax-activation, parameters were varied

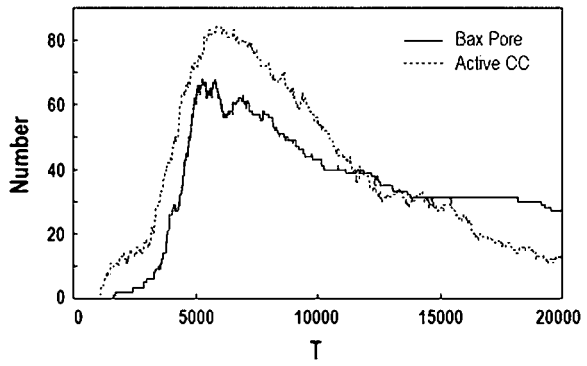

FIGURE 4 Changes of the initial ratio of Bax to CC and relative parameters reverse the ratio of Bax pores to active CC. 3200 Bcl2, 500 InBax, 200 Activator, 80 Enabler, 100 CC, and 3200 other proteins scattered on the MOM as the initial condition. K_{21} is enlarged to 100, K_{22} is reduced to 15. Other constants are given the same as in Table 3. Active CC constitute the major parts of the pores in this simulation.

systematically within a certain range (for example, k_1 was varied from 0.1 to 5.0, Fig. 6). The results reveal that bistability exists in a large region of parameter space. Further analyses with the translocation of Bax or Bcl2 as stimuli F and bifurcation parameters show bistability as well (Fig. 7).

The going-up and coming-down analysis with stimuli F as the parameter is performed by solving the ODEs (using MatLab 6.5): F is varied along two directions (going-up and coming-down, the former with 2×10^{-4} mM InBax as initialization and the latter with 2×10^{-4} mM AcBax as initialization) and the amounts of AcBax in final steady states (we calculated up to 50,000 steps) are plotted in Fig. 8 *a*. A hysteretic phenomenon exists during this simulation. In a system that is initially inactive with increasing stimuli F, the ratio of AcBax to Total Bax remains near zero until it passes a point at $\sim F = 0.32$, where a sudden jump is seen. However, when we reduce the stimuli F back, additional decrease is needed to set this system back to the inactive state. This result is consistent with Fig. 5 in which the on-state loses its stability with a sudden decrease of AcBax level when the stimuli F comes below a restriction point $F = 0.15$. Our results indicate that a memory of the transient stimuli is produced by the core module of Bax-activation.

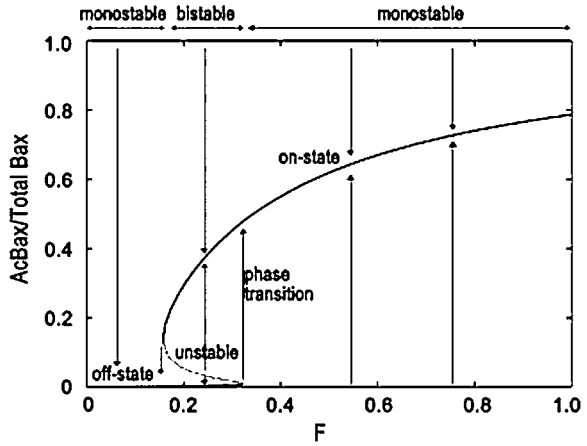

FIGURE 5 Bifurcation diagram of the core module of Bax activation as a function of the stimuli F. Translocation of Activator is taken as the stimuli F ($F_1 = F_3 = 0$, F_2 varies from 0 to 1). The limit points for saddle-node bifurcation are at $F = 0.15$ and 0.32. The arrows indicate the equilibrium concentrations reached when starting from any point in the diagram.

CA modeling

Noise is an important factor in the function of biological reaction networks, as simulation studies have abundantly demonstrated (18,53). In real reaction systems, stochastic fluctuations of Bax-activation may destroy the bistable behavior of the core module of Bax-activation effectively. For instance, any perturbation of Bax-activation higher than the unstable state will send the system up to the on-state from the off-state. So, if the system is too sensitive to noise, no bistability will exist. This raises a concern of whether bistability exits if stochastic fluctuations are taken into account. Here CA modeling gives an opportunity to construct such a stochastic model.

The interaction rules in Table 2 were modified to realize the core module of Bax-activation (the rate of Bax-polymerization is set to zero). We performed simulations in a grid of 50×50 squares (a quarter of the MOM), on which we uniformly scattered 800 AcBax (or InBax), 400 Bcl2, and 800 Other molecules as initialization. The amount of translocated Activator is taken as the apoptotic stimulus. Temporal evolution of the amount of AcBax with the given stimuli can be simulated. We performed going-up and coming-down analysis as follows: stimuli were varied along two directions (going-up and coming-down, the former with 800 InBax as initialization and the latter with 800 AcBax as initialization) and the amounts of AcBax in final steady states (we calculated up to 30,000 steps) are plotted in Fig. 8 *b*.

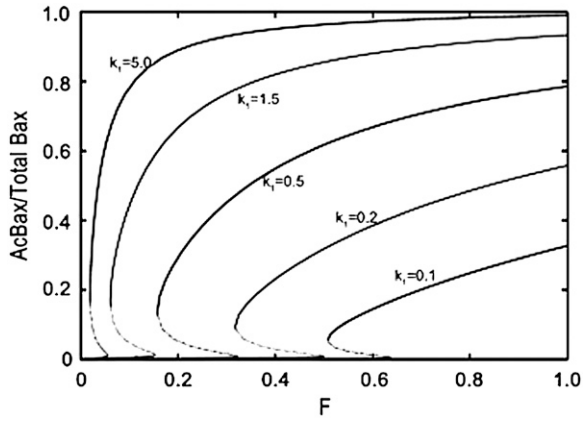

FIGURE 6 Bifurcation diagram illustrating the role of k_1. Bistability exists in a large region of parameter k_1. Translocation of Activator is taken as the apoptosis stimuli F ($F_1 = F_3 = 0$, F_2 varies from 0 to 1).

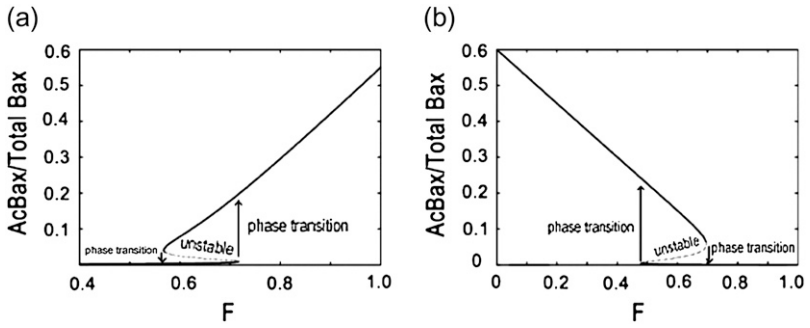

FIGURE 7 The module of Bax activation shows bistabilities with the concentrations of (*a*) total Bax and (*b*) total Bcl2 as the bifurcation parameters. (*a*) Translocation of Bax is taken as the stimuli F ($F_2 = F_3 = 0$, F_1 varies from 0 to 1). $Act_{\text{mito}} = 0.4 \times 10^{-4}$ mM, $Bax_{\text{mito}} = 0$ mM, $Bcl2_{\text{mito}} = 1 \times 10^{-4}$ mM, and $Bax_{\text{cytosol}} = 2 \times 10^{-4}$ mM are set as initial conditions. (*b*) Translocation of Bcl2 is taken as the stimuli F ($F_1 = F_2 = 0$, F_3 varies from 0 to 1). $Act_{\text{mito}} = 0.3 \times 10^{-4}$ mM, $Bax_{\text{mito}} = 2 \times 10^{-4}$ mM, $Bcl2_{\text{mito}} = 0$ mM, and $Bcl2_{\text{cytosol}} = 1 \times 10^{-4}$ mM are set as initial condition.

Increasing stimuli induce a sudden jump of the AcBax steady level and it takes additional decreases of stimuli to bring the system back to the off-state. Therefore, bistability of the core module of Bax-activation exists in both our deterministic and stochastic models.

Coupling with Bax-polymerization

The bistable character of Bax-activation can relay a digital, all-or-none signal to downstream events, e.g., MAC formation and MOMP. It is therefore proposed to be a possible explanation for the switchlike behavior of apoptosis. However, there still remain two questions: first, the on-state and off-state of the Bax-activation can be realized only in a limited parameter range, whereas outside of this range only one of them prevails. It is uncertain whether parameter values in physiological conditions would meet these restrictive constraints to make the module bistable. Second, the bistable module of Bax-activation can act as a toggle switch that is bidirectional, but this is not the case in apoptosis induction. In other words, the module of Bax-activation lacks irreversibility. These questions indicate that bistability of the Bax-activation module is unlikely to be the sole mechanism behind bioswitching of apoptosis induction.

Bax-polymerization into clusters, which could represent protein-conducting pores, is the very end of the MOMP regulatory network (34). Thus both models mentioned above are extended to study the effects of Bax-polymerization on the dynamics of Bax-activation. In the ODE model, four AcBax are assumed to aggregate into a tetramer and this process is set to be irreversible. The strength of CA modeling was taken to enable more realistic modeling where AcBax can aggregate into big clusters in a partly reversible process (for details, see Table 3). Again this was applied in the going-up and coming-down analysis to get the dynamics of the Bax-activation.

The cooperativity of Bax-polymerization can play a central role in providing a decisive and irreversible transition in Bax-activation against noise. In the ODE model (Fig. 9 *a*), F is increased from 0 to 1 and upon passing a restriction point, the amount of AcBax is lifted with a sudden jump in a similar pattern as in Fig. 8 *a*. However, it cannot be recovered to an off-state even when F has been reduced to 0. A transition from a toggle switch to a one-way switch takes place when Bax-polymerization is incorporated to the core module of Bax-activation. This one-way switch mechanism can give a reasonable explanation for the irreversibility of apoptosis induction. Another apparent difference is that the AcBax level of the on-state is lifted to a higher level when coupled with Bax-polymerization. With respect to robustness against noise, this scenario has advantages over the situation where the AcBax level of the on-state is lower because the barrier that separates the off-state and on-state of Bax-activation is now enlarged. All these make a robust one-way switch of Bax-activation. A similar conclusion can also be drawn from the results of the CA simulation (Fig. 9 *b*).

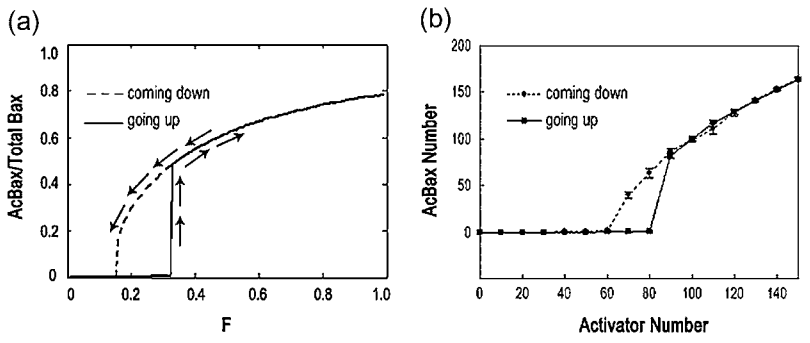

FIGURE 8 Going-up and coming-down analysis with stimuli F as parameter of the core module of Bax activation. (*a*) In the ODEs modeling of the core module of Bax activation, the amount of Activator, which represents the stimuli F ($F_1 = F_3 = 0$, F_2 varies from 0 to 1), is varied along two directions (going-up and coming-down) and the AcBax numbers of final steady states are plotted versus F. (*b*) In the CA modeling of the core module of Bax activation, the amount of Activator, which represents the stimuli F, is varied along two directions (going-up and coming-down) and the AcBax numbers of final steady states are plotted versus the number of Activator (mean ± SE of three independent simulation results). The reaction rate constants are given as $K_1(300)$, $K_2(12)$, $K_3(800)$, $K_4(3)$, $K_5(1000)$, $K_6(1)$, $K_7(500)$, and $K_8(300)$. All other rate constants are set to be zero.

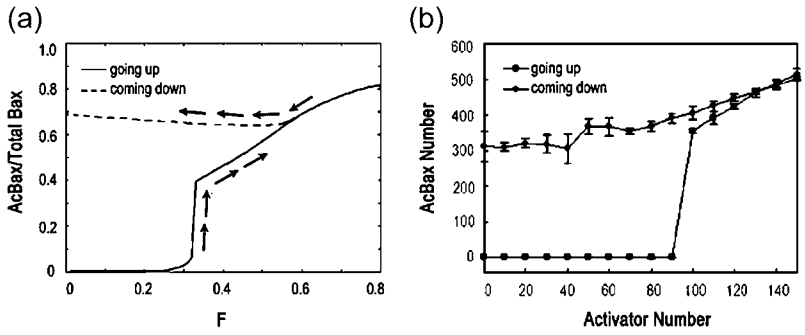

FIGURE 9 Coupling to the Bax polymerization makes a one-way-switch. (*a*) Extended ODE model considering Bax polymerization. The amount of Activator, which represents the stimuli F ($F_1 = F_3 = 0$, F_2 varies from 0 to 1), is varied along two directions (going-up and coming-down) and the AcBax numbers of final steady states are plotted versus F. (*b*) Extended CA model, given is the mean ± SE of three independent simulation results.

CONCLUSION

In the present study, a systems biology approach was used to understand dynamic processes in apoptosis induction. Both ODE and CA models for mitochondrial apoptosis regulatory network were developed based on qualitative and semiquantitative knowledge. A mitochondrial switch of Bax-activation was proposed to be one of the mechanisms for the all-or-none, irreversible behavior of cells in response to apoptotic stimuli.

The purpose of this article is to look into the mitochondrial apoptosis regulatory network. A self-amplification process of Bax-activation is reported in the literature and observed during the CA simulation of the mitochondrial apoptosis regulatory network. This is due to a positive feedback embedded in the interaction network of Bcl-2 family proteins. To examine whether the positive feedback is strong enough to bring about bistability, a core module of Bax-activation was constructed by both ODE and CA modeling. Bifurcation analysis and further studies revealed that bistability does exist and seems to be an inherent characteristic of the core module. It acts a toggle switch governing Bax-activation and changes to a one-way switch with the cooperation of Bax-polymerization, which strongly improves its robustness against stochastic fluctuations in physiological conditions.

From the simulation results, it can be concluded that the remarkable activation and polymerization of Bax is a checkpoint of the cell fate decision. The idea that the point at which epithelial cells undergoing anoikis (a kind of apoptosis) have irreversibly committed to apoptosis equates to Bax-activation is well in accord with this conclusion. Epithelial cells can be rescued from anoikis even after Bax has distributed to the MOM, with a small part of them activated at an early stage. However once Bax-polymerization occurs on MOM, cells cannot be rescued (13,33). This implies that the commitment of apoptosis occurs after Bax translocation but before Bax-polymerization.

A further conclusion drawn from the simulation results is that two states of cells could possibly coexist under a given stimulus. This kind of bimodal population distribution is common in bistable systems. A recent study by Nair et al. (12) matches surprisingly well with this conclusion. Upon examination of a population of cells undergoing oxidative stress at single cell level, they detected a bifurcation of cell fates into two states, either cell death or survival. The choice of individual cells between these two exclusive states is suggested to be a stochastic process, which is still lacking elucidation. The mechanism proposed in this article gives a possible explanation.

The stochastic modeling approach of cellular automaton was displayed, which aided in uncovering the inherent function of the mitochondrial apoptosis regulatory network in a stochastic way. The CA approach has been successfully employed for many years in various fields (54). Noise arises because of its particulate or discrete nature. The stochasticity also arises from the high level of reversibility for reactions. CA-based simulations of biochemical networks, especially for the apoptosis regulatory network, were scarce until recently. Siehs et al. (20) simulated the time evolution of Bcl-2 family proteins using discrete time and space variables in a Lattice Molecular Automaton (LMA). This was the first attempt to analyze the apoptosis regulatory mechanism in a discrete, stochastic model. Their studies would have been more realistic if they had considered more detailed interactions of Bcl-2 family proteins. A crucial feature of our model that differs from LMA is that it utilizes Brownian motion to mimic the movements of molecules at the single mitochondrion level. This significant dynamic simplification potentially allows very long timescales and large numbers of entities or reactions to be modeled on a personal computer. Also, construction of CA models is mainly based on qualitative and semiquantitative knowledge of biochemical reactions, molecule numbers, and kinetic rates and can be easily expanded into a complex model as long as more qualitative and quantitative data is obtained.

It should be noted that this study has only examined the mitochondrial apoptosis regulatory network, which is a small part of the complex network of apoptosis regulation. The Bax-activation switch proposed here should not be the sole mechanism of the all-or-none, irreversible character of apoptosis. A lot of work has already been done focused on positive feedbacks (both short-term and long-term) and cooperativities that can give rise to bistability. These upstream and downstream events should undoubtedly be described to gain a systematic understanding of this complex network. Furthermore, the simulations performed here are taken at

single mitochondrion level and the copy numbers of different proteins are definite. However, most experimental studies have been performed using a population of cells, with different number of mitochondria in each cell with diverse copy numbers of different proteins. This kind of system noise is neglected in our models. Another limitation of this study is that certain parameters used in the models are chosen to reflect the experimentally known features. It is adequate when only qualitative and semiquantitative characters are discussed. However, we should expect that much of the numerically known or estimated quantities can be made used for exact construction of the network as more experimental data are obtained.

Notwithstanding these limitations, our models take a very important step for carrying out both deterministic and stochastic modeling of the apoptosis regulatory network, in particular of mitochondrial regulatory events. This study suggests that the module of Bax-activation coupling with Bax-polymerization can act as a one-way switch governing the all-or-none and irreversible behavior of apoptosis induction.

We thank Edward Kalmykov (Department of Biochemistry, University of Texas Health Science at San Antonio) for grammatical correction of the article.

This study was supported by the National Natural Science Foundation of China (project No. 30571538 and 20477016), the Natural Science Foundation of Jiangsu Province of China (project No. BK2006120), and the 111-PROJECT.

REFERENCES

1. Milo, R., S. Shen-Orr, S. Itzkovitz, N. Kashtan, D. Chklovskii, and U. Alon. 2002. Network motifs: simple building blocks of complex networks. *Science*. 298:824–827.
2. Swat, M., A. Kel, and H. Herzel. 2004. Bifurcation analysis of the regulatory modules of the mammalian G1/S transition. *Bioinformatics*. 20:1506–1511.
3. Tyson, J. J., K. Chen, and B. Novak. 2001. Network dynamics and cell physiology. *Nat. Rev. Mol. Cell Biol.* 2:908–916.
4. Gombert, A. K., and J. Niesen. 2000. Mathematical modeling of metabolism. *Curr. Opin. Biotechnol.* 11:180–186.
5. Varner, J., and D. Ramkrishna. 1999. Mathematical models of metabolic pathways. *Curr. Opin. Biotechnol.* 10:146–150.
6. Fussenegger, M., J. E. Bailey, and J. Varner. 2000. A mathematical model of caspase function in apoptosis. *Nat. Biotechnol.* 18:768–774.
7. Castiglione, F., and S. Succi. 2005. Simulating the G-protein cAMP pathway with a two-compartment reactive lattice gas. *Theor. Biosci.* 123:413–429.
8. Wishart, D. S., R. Yang, D. Arndt, P. Tang, and J. Cruz. 2005. Dynamic cellular automata: an alternative approach to cellular simulation. *In Silico Biol.* 5:1–23.
9. Wurthner, J. U., A. K. Mukhopadhyay, and C. Peimann. 2000. A cellular automaton model of cellular signal transduction. *Comput. Biol. Med.* 30:1–21.
10. Shimizu, T. S., S. V. Aksenov, and D. Bray. 2003. A spatially extended stochastic model of the bacterial chemotaxis signaling pathway. *J. Mol. Biol.* 329:291–309.
11. Goldstein, J. C., R. M. Kluck, and D. R. Green. 2000. A single cell analysis of apoptosis: ordering the apoptotic phenotype. *Ann. N. Y. Acad. Sci.* 926:132–141.
12. Nair, V. D., T. Yuen, C. W. Olanow, and S. C. Sealfon. 2004. Early single cell bifurcation of pro- and antiapoptotic states during oxidative stress. *J. Biol. Chem.* 279:27494–27501.
13. Valentijn, A. J., A. D. Metcalfe, J. Kott, C. H. Streuli, and A. P. Gilmore. 2003. Spatial and temporal changes in Bax subcellular localization during anoikis. *J. Cell Biol.* 162:599–612.
14. Bentele, M., I. Lavrik, M. Ulrich, S. Stosser, D. W. Heermann, H. Kalthoff, P. H. Krammer, and R. Eils. 2004. Mathematical modeling reveals threshold mechanism in CD95-induced apoptosis. *J. Cell Biol.* 166:839–851.
15. Eissing, T., H. Conzelmann, E. D. Gilles, F. Allgower, E. Bullinger, and P. Scheurich. 2004. Bistability analyses of a caspase activation model for receptor-induced apoptosis. *J. Biol. Chem.* 279:36892–36897.
16. Bagci, E. Z., Y. Vodovotz, T. R. Billiar, G. B. Ermentrout, and I. Bahar. 2005. Bistability in apoptosis: roles of Bax, Bcl-2 and mitochondrial permeability transition pores. *Biophys. J.* 90:1546–1559.
17. Green, D. R., and G. Kroemer. 2005. Pharmacological manipulation of cell death: clinical applications in sight? *J. Clin. Invest.* 115:2610–2617.
18. Rao, C. V., D. M. Wolf, and A. P. Arkin. 2002. Control, exploitation and tolerance of intracellular noise. *Nature*. 420:231–237.
19. Tian, T., and K. Burrage. 2006. Stochastic models for regulatory networks of the genetic toggle switch. *Proc. Natl. Acad. Sci. USA*. 103: 8372–8377.
20. Siehs, C., R. Oberbauer, G. Mayer, A. Lukas, and B. Mayer. 2002. Discrete simulation of regulatory homo- and heterodimerization in the apoptosis effector phase. *Bioinformatics*. 18:67–76.
21. Saikumar, P., Z. Dong, V. Mikhailov, M. Denton, J. M. Weiberg, and M. A. Venkatachalam. 1999. Apoptosis: definition, mechanisms, and relevance to disease. *Am. J. Med.* 107:489–506.
22. Loo, G., X. Saelens, M. Gurp, M. MacFarlane, S. Martin, and P. Vandenabeele. 2002. The role of mitochondrial factors in apoptosis: a Russian roulette with more than one bullet. *Cell Death Differ.* 9: 1031–1042.
23. Letai, A. 2005. Pharmacological manipulation of Bcl-2 family members to control cell death. *J. Clin. Invest.* 115:2648–2655.
24. Schinzel, A., T. Kaufmann, and C. Borner. 2003. Bcl-2 family members: intracellular targeting, membrane-insertion, and changes in subcellular localization. *Biochim. Biophys. Acta*. 1644:95–105.
25. Bouchier-Hayes, L., L. Lartigue, and D. D. Newmeyer. 2005. Mitochondria: pharmacological manipulation of cell death. *J. Clin. Invest.* 115:2640–2647.
26. Tsujimoto, Y. 2003. Cell death regulation by the bcl-2 protein family in the mitochondria. *J. Cell. Physiol.* 195:158–167.
27. Cartron, P. F., T. Gallenne, G. Bougras, F. Gautier, F. Manero, P. Vusio, K. Meflah, F. M. Vallette, and P. Juin. 2004. The first alpha helix of Bax plays a necessary role in its ligand-induced activation by the BH3-only proteins Bid and PUMA. *Mol. Cell.* 16:807–818.
28. Marani, M., T. Tenev, D. Hancock, J. Downward, and N. R. Lemoine. 2002. Identification of novel isoforms of the BH3 domain protein Bim which directly activate Bax to trigger apoptosis. *Mol. Cell. Biol.* 22: 3577–3589.
29. Esposti, M. D., and C. Dive. 2003. Mitochondrial membrane permeabilization by Bax/Bak. *Biochem. Biophys. Res.* 304:455–461.
30. Ruffolo, S. C., and G. C. Shore. 2003. Bcl-2 selectively interacts with the Bid-induced open conformer of BAK, inhibiting BAK auto-oligomerization. *J. Biol. Chem.* 278:25039–25045.
31. Yi, X., X. Yin, and Z. Dong. 2003. Inhibition of Bid-induced apoptosis by Bcl-2, tBid insertion, Bax translocation, and Bax/Bak oligomerization suppressed. *J. Biol. Chem.* 278:16992–16999.
32. Letai, A., M. C. Bassik, L. D. Walensky, S. Weiler, and J. Korsmeyer. 2002. Distinct BH3 domains either sensitize or activate mitochondrial apoptosis, serving as prototype cancer therapeutics. *Cancer Cell.* 2:183–192.
33. Gilmore, A. P., A. D. Metcalfe, L. H. Romer, and C. H. Streuli. 2000. Integrin-mediated survival signals regulate the apoptotic function of

Bax through its conformation and subcellular localization. *J. Cell Biol.* 149:431–445.

34. Dejean, L. M., S. Martinez-Caballero, S. Manon, and K. W. Kinnally. 2006. Regulation of the mitochondrial apoptosis-induced channel, MAC, by Bcl-2 family proteins. *Biochim. Biophys. Acta.* 1762: 191–201.
35. Saito, M., S. J. Korsmeyer, and P. H. Schlesinger. 2000. Bax-dependent transport of cytochrome *c* reconstituted in pure liposomes. *Nat. Cell Biol.* 2:553–555.
36. Nechushtan, A., C. L. Smith, I. Lamensdorf, S. Yoon, and R. J. Youle. 2001. Bax and Bak coalesce into novel mitochondria-associated clusters during apoptosis. *J. Cell Biol.* 153:1265–1276.
37. Verrier, F., B. Mignotte, G. Jan, and C. Brenner. 2003. Study of PTPC composition during apoptosis for identification of viral protein target. *Ann. N. Y. Acad. Sci.* 1010:126–142.
38. Zamzami, N., and G. Kroemer. 2001. The mitochondrion in apoptosis: how Pandora's box opens. *Nat. Rev. Mol. Cell Biol.* 2:67–71.
39. Alber, M. S., M. A. Kiskowski, J. A. Glazier, and Y. Jiang. 2003. On cellular automaton approaches to modeling biological cells. *In* Mathematical Systems Theory in Biology, Communication, and Finance. J. Rosenthal, and D. S. Gilliam, editors. Springer-Verlag, New York.
40. Minton, A. P. 2001. The influence of macromolecular crowding and macromolecular confinement on biochemical reactions in physiological media. *J. Biol. Chem.* 276:10577–10580.
41. Chen, C., J. Cui, S. Zhang, and P. Shen. 2006. Cellular automaton simulation of the Bcl-2 family proteins regulated mitochondrial outer membrane permeabilization. *In* The Study of Intelligent Computing Theory and Methodology in Bioinformatics. D. Huang et al., editors. USTC Publishers/China, Hefei. 194–200.
42. Kuwana, T., M. R. Mackey, G. Perkins, M. H. Ellisman, M. Latterich, R. Schneiter, D. R. Green, and D. D. Newmeyer. 2002. Bid, Bax and lipids cooperate to form supramolecular openings in the outer mitochondrial membrane. *Cell.* 111:331–342.
43. Hua, F., M. G. Cornejo, M. H. Cardone, C. L. Stokes, and D. A. Lauffenburger. 2005. Effects of Bcl-2 levels on Fas signaling induce Capase-3 activation: molecular genetic tests of computational model predictions. *J. Immunol.* 175:985–995.
44. Bhattacharyya, A., D. Mandal, L. Lahiry, G. Sa, and T. Das. 2004. Black tea protects immunocytes from tumor-induced apoptosis by changing Bcl-2/Bax ratio. *Cancer Lett.* 209:147–154.
45. Tirado, O. M., S. Mateo-Lozano, and V. Notario. 2005. Rapamycin induces apoptosis of JN-DSRCT-1 cells by increasing the Bax:Bcl-Xl ratio through concurrent mechanisms dependent and independent of its mTOR inhibitory activity. *Oncogene.* 24:3348–3357.
46. Childs, A. C., S. L. Phaneuf, A. J. Dirks, T. Philips, and C. Leeuwenburgh. 2002. Doxorubicin treatment in vivo causes cytochrome *c* release and cardiomyocyte apoptosis, as well as increased mitochondrial efficiency, superoxide dismutase activity, and Bcl-2:Bax ratio. *Cancer Res.* 62:4595–4598.
47. Chang, L. K., and E. M. Johnson. 2002. Cyclosporin A inhibits caspase-independent death of NGF-deprived sympathetic neurons: a potential role for mitochondrial permeability transition. *J. Cell Biol.* 157:771–781.
48. Shimizu, S., Y. Matsuoka, Y. Shinohara, Y. Yoneda, and Y. Tsujimoto. 2001. Essential role of voltage-dependent anion channel in various forms of apoptosis in mammalian cells. *J. Cell Biol.* 152:237–250.
49. Adachi, M., H. Higuchi, S. Miura, T. Azuma, S. Inokuchi, H. Saito, S. Kato, and H. Ishii. 2004. Bax interacts with the voltage-dependent anion channel and mediates ethanol-induced apoptosis in rat hepatocytes. *Am. J. Physiol. Gastrointest. Liver Physiol.* 287:695–705.
50. Terada, S., T. Kumagai, N. Yamamoto, A. Ogawa, J. Ishimura, T. Fujita, E. Suzuki, and M. Miki. 2003. Generation of a novel apoptosis-resistant hepatoma cell line. *J. Biosci. Bioeng.* 95:146–151.
51. Tan, C., P. J. Dlugosz, J. Peng, Z. Zhang, S. M. Lapolla, S. M. Plafker, D. W. Andrews, and J. Lin. 2006. Auto-activation of the apoptosis protein Bax increases mitochondrial membrane permeability and is inhibited by Bcl-2. *J. Biol. Chem.* 281:14764–14775.
52. Ferrell, J. M., and W. Xiong. 2001. Bistability in cell signaling: how to make continuous processes discontinuous, and reversible processes irreversible. *Chaos.* 11:227–238.
53. Hasty, J., J. Pradines, M. Dolnik, and J. J. Collins. 2000. Noise-based switches and amplifiers for gene expressions. *Proc. Natl. Acad. Sci. USA.* 97:2075–2080.
54. Chopard, B., and M. Droz. 1998. Cellular Automata Modeling of Physical Systems. Cambridge University Press, Cambridge, UK.